The impact of wakes from neighboring wind farms on the production of the IJmuiden Ver wind farm zone

December 23, 2022

Peter Baas[1] **and Remco Verzijlbergh**[1,2]

[1]Whiffle, Molengraaffsingel 8, 2629 JD Delft, The Netherlands
[2]Delft University of Technology, Department of Engineering Systems & Services, Jaffalaan 5, 2628 BX Delft, the Netherlands

ABSTRACT

This explorative study examines the potential impact of surrounding wind farms on the production of the planned 4 GW IJmuiden Ver wind farm with atmospheric large-eddy simulation. We compared production numbers of a simulation with the IJmuiden Ver wind farm in isolation with those of a simulation with all surrounding wind farms included. Results of both simultions were compared to free-stream production numbers. The modeling results indicate that the energy production of the future wind farm of IJmuiden Ver may experience significant production losses from wake effects of upstream wind farms. On a yearly basis the production deficit could amounts to 4 %. For wind speed between 6 and 12 m/s this number increases to 10 %. The production deficits resulting from upstream wind farms show a strong dependency on wind direction. When only considering wind directions with upstream wind farms ('disturbed' sectors) the production deficit may even increase to 20 % in stably-stratified conditions. Inspection of spatial fields reveal complex patterns of both wind farm wakes and flow accelerations along the sides of individual wind farms. The results of the present study suggest that with the rapid increase of offshore wind energy capacity farm-to-farm interactions cannot be ignored.

1 Introduction

As part of the transition to renewable energy sources, the European offshore wind energy capacity is expanding rapidly. For example, the offshore wind energy capacity in Dutch, Belgian, Danish and German parts of the North Sea is anticipated to reach the 65 GW mark in the year 2030 and 150 GW in the year 2050 [The Esbjerg Declaration, 2022]. The European-wide target for offshore wind in 2050 is 300 GW [European Commission, 2020]. While the original Dutch Roadmap for 2030 targeted an installed capacity of 10 GW, revisited ambitions are aiming for 20 GW in that year ([Rijksoverheid, 2021]). Presently, the total installed capacity in the Dutch EEZ ammounts to 4 GW. These numbers highlight the enormous acceleration of the offshore wind energy capacity in the coming years.

Ten years ago, the largest offshore windfarms had a capacity of around 500 MW. Nowadays, this number has increased to 1500 MW and before the year 2030, wind farms of 4000 MW will be no exception. But even wind farms of considerably smaller size can produce significant wake areas that can extend tens of kilometers (eg [Hasager et al., 2015], [Platis et al., 2018], [Schneemann et al., 2020]). As the number of wind farms will increase strongly, the distance between wind farms will become smaller. This will especially hold for preferrable areas that are, for example, not too far offshore with limited water depth and good wind climate. All these factors emphasize the importance of knowledge on how inter-windfarm wakes impact the power production of downstream wind farms. Farm-to-farm interations may have substantial adverse economical consequences ([Lundquist et al., 2019]). Better insight in inter-wind farm wake effects is especially relevant, since up till today the impact of inter-wind farm wake effects are largely ignoreed in AEP projections.

The present work aims to provide an estimate the impact of neighboring wind farms on the power production of the planned IJmuiden Ver wind farm, for which a tender is expected to open in 2023 [RVO, 2022]. This 4000 MW wind farm is a nice example to study inter-windfarm wake effect as it will be surrounded by multiple other large wind farms in different directions. Typically the distance beteen the neighboring wind farms and IJmuiden Ver will be in the order of 10 to 20 km.

To address the impact of the surrounding wind farms on IJmuiden Ver we simulate one year of actual weather with the GRASP (GPU-Resident Atmospheric Simulation Platform) LES model. This is done by driving the LES with data from

ECMWF's ERA5 reanalysis dataset [Hersbach et al., 2020]. In this way, we obtain representative distributions of, for example, wind speed, stability, and baroclinicity in a natural way [Schalkwijk et al., 2015]. Three simulation are performed. In one simulation we model the IJmuiden Ver wind farm in isolation, while a second simulation also includes the neighboring wind farms. The difference between these simulations provides an estimate of the impact of the upstream wind farms on the IJmuiden Ver power production. A third simulation provides an estimate of free-stream production numbers. The output of the model further allows us to assess the spatial variability of the impact of neighboring wind farms and how this impact depends on wind speed and atmospheric stability.

This report is organized as follows. Section 2 describes the modeling technique and the simulation set-up, Section 3 gives an overview of the wind farms that are included, such as locations, assumed layouts and turbine types. Section 4 presents the main results. After discussing the results in Section 5, the conclusions are summarized in Section 6.

2 Model description and simulation strategy

2.1 Model description

The model simulations are carried out with the GPU-Resident Atmospheric Simulation Platform (GRASP). The origin of GRASP can be traced back to the Dutch Atmospheric Large Eddy Simulation model (DALES), which is extensively described in [Heus et al., 2010].

To overcome the barrier of the large computational costs that have long prohibited the use of LES in operational weather forecasting, the DALES model was translated to a code that runs most of its computational routines on GPUs [Schalkwijk et al., 2012]. In its stand-alone version, GRASP uses a traditional Charnock relation for its lower boundary condition over water surfaces.

For modeling the impact of wind turbines on the flow, GRASP uses an actuator-disk parametrization as described by [Meyers and Meneveau, 2010] and [Calaf et al., 2010]). This parametrization only needs information about the power curve, thrust curve, rotor diameter and hub height. The parametrization calculates the drag forces (using the thrust curve) and rotational forces (using the power curve) based on the local wind speed, taking the actual induction into account. Individual yaw control based on the local wind direction is applied to the turbines.

In the present set-up, GRASP uses periodic boundary conditions. To prevent the recirculation of wind-farm wakes, we make use of a concurrent-precursor simulation [Stevens et al., 2014]. This is a simulation without wind turbines that runs in parallel with the 'actual' simulation. Over the boundary region the values of the 'actual' simulation are nudged towards the precursor simulation. A schematic overview of this set-up is shown in Figure 1.

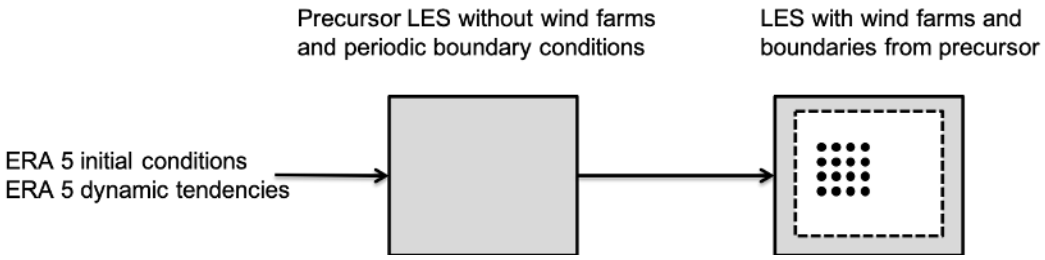

Figure 1. Schematic view of ERA5 boundary conditions, a precursor simulation and a nested domain.

For more details on the LES model we refer to [Baas et al., 2022].

2.2 Simulation strategy

For the present study, the entire year of 2015 has been simulated with GRASP. The large-scale boundary conditions (i.e. the synopic 'weather') are provided by ECMWF's ERA5 reanalysis dataset [Hersbach et al., 2020]. The year-long simulation consists of concatenated daily simulations with a spin-up time of 2 hours. For each day, GRASP is initialized at 22 h (UTC) the previous day. Model output valid between 0 and 24 h (UTC) is used for the analysis.

The modeling domain was set-up to include the IJmuiden Ver wind farm and its neighboring wind farms. The domain consists of 1024 x 1024 x 48 grid points. The horizontal grid spacing is 140 m, the lowest grid box has a height of 32.5 m. The horizontal domain size extends to 143.36 km. Vertical grid stretching was applied to obtain a domain height of 3000 m. The model domain is centred around 52.881° N and 3.337° E. The domain includes the location of the MeteoMast IJmuiden, which was operational during the simulated year.

Compared to other LES studies such as [Maas and Raasch, 2022], the horizontal resolution of 140m is relatively coarse. This choice results from a trade-off between computational cost and accuracy. Using the same model, [Baas et al., 2022] assess

the sensitivity to resulution and domain settings on wind farm production numbers and find only a modest impact. In particular, they report that relative differences between various wind farm scenarios or layouts are very small. As such, we argue that the present set-up allows for a reliable first-estimate of additional losses due to neighboring wind farms.

Three simulations are performed simultaneously:

1. A concurrent-precursor simulation that provides the boundary conditions for the actual simulations. In this simulation, so-called 'thrustless turbines' are added for the IJmuiden Ver wind farm. These turbines do produce power, but do not excert any drag on the flow. As such, they do not produce wake effects and their production can be regarded as free-stream production. In the following, we refer to this simulation as *SIM-FS*.

2. A simulation containing only the IJmuiden Ver wind farm (*SIM-ISO*).

3. A simulation containing both IJmuiden Ver and the surrounding wind farms (*SIM-ALL*). Details of the included wind farms and applied turbines are presented in Section 3.

As a basic validation of the model's capability to represent the local wind conditions, Fig. 2a compares modeled wind speed at a height of 92 m with observations from the MeteoMast IJmuiden. The correspondence between model and tower observations are satisfactory, with error metrics within the expected range for wind resource assessments. Figure 2b shows the distribution of the modeled 92m wind speed, with a Weibull function fitted to the data. For comparison, grey dots indicate the distribution of the observations. Figure 2c presents the (modeled) wind rose, indicating that southwesterly winds have the highest frequency of occurrence and are generally stronger than winds from other sectors.

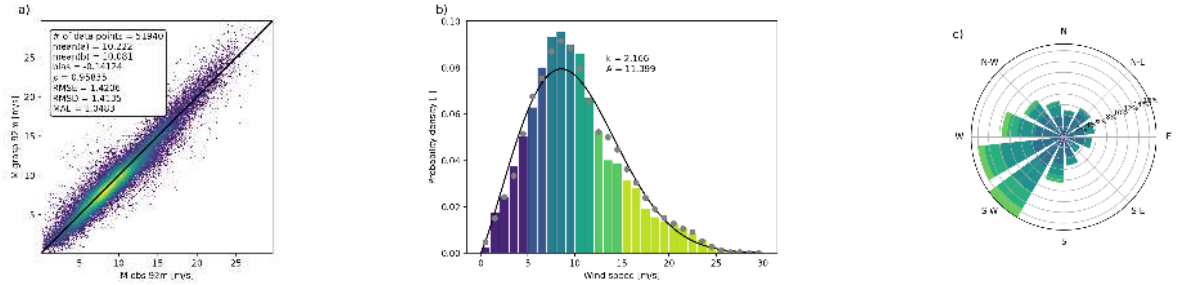

Figure 2. Validation results of GRASP vs. offshore tall mast IJmuiden. a) Modeled versus observed wind speed at 92 m. b) Weibull plot of GRASP 92m wind speed. Grey dots represent the observations. c) Modeled wind rose at 92 m.

3 Overview of wind farms and turbine specifications

The planned IJmuiden Ver wind farm will be surrounded by multiple other Dutch and Britsh wind farms. Figure 3 gives an overview of the modeling domain and all the wind farms that are included in this study. In Table 1 more details for each of the wind farms are listed. For IJmuiden Ver, the 268 turbines are equally distributed over the four sites ('kavels'), with each site containing 67 turbines. All wind farms are planned in reality and we use actual site boundaries based on publicly available data. It should be noted that plans and roadmaps are subject to change and that, as such, the final configuration of wind farms in this area will probably differ from the one used in the present study. Also, in reality even more wind farms are planned in the area covered by our model domain, for instance the wind farms of Lagelander en the northern part of Nederwiek. Just outside the modeling domain the Hollandse Kust Noord, Hollandse Kust Zuid and other Britsh wind farms are located. Nevertheless, the results based on the present layout will provide usefull first insights into the potential impact of neighboring wind farms on IJmuiden Ver.

As no individual turbine coordinates are available, we distributed the required number of turbines uniformly over the subsequent wind farm areas using an iterative repulsion method [Witkin and Heckbert, 2005]. For each wind farm, the number of turbines is given by dividing the anticipated installed capacity by the capacity of the individual turbines (see Table 1). Two turbine types are applied. For wind farms that will be commissioned in the next few years the 10 MW DTU reference turbine has been selected. For wind farms that will become operational around 2030 we use the 15 MW IEA reference turbine. Power- and thrustcurves of the IEA15 and DTU10 turbines are given in Figure 4. Turbine data are taken from https://nrel.github.io/turbine-models/Offshore.html.

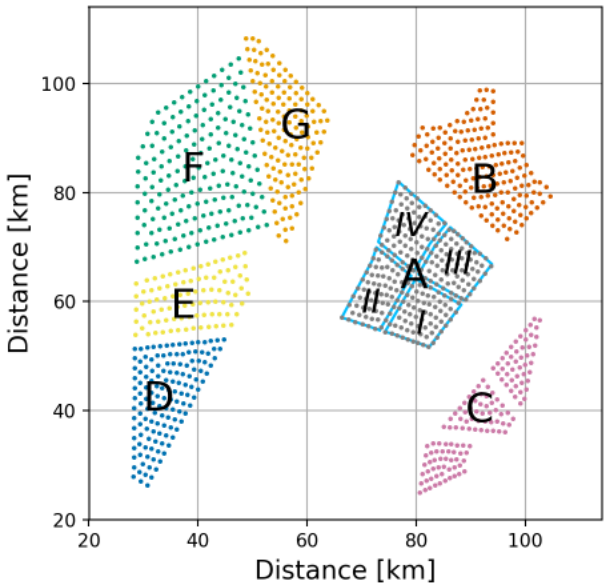

Figure 3. Overview of simulated wind farms. Letters correspond to the wind farm id's in Table 1. The four separate sites ('kavels') of the IJmuiden Ver wind farm are indicated with numbers *I* to *IV*. The distances along the axes correspond to locations in the computational domain.

Id	Name	Turb. type	Hub height [m]	r [m]	P_rated [WM]	N [-]	P_installed [MW]
A	IJmuiden Ver	IEA_15MW_240RWT	150	120	15	268	4020
B	IJmuiden Ver North	IEA_15MW_240RWT	150	120	15	167	2505
C	HKW	IEA_15MW_240RWT	150	120	15	141	2105
D	East Anglia Hub - Three	DTU_10MW_178RWT	119	89	10.6	140	1484
E	Norfolk Vanguard East	DTU_10MW_178RWT	119	89	10.6	90	954
F	Norfolk Boreas	DTU_10MW_178RWT	119	89	10.6	180	1908
G	Nederwiek Zuid	IEA_15MW_240RWT	150	120	15	140	1995

Table 1. Overview of modeled wind farms, including basic turbines characteristics.

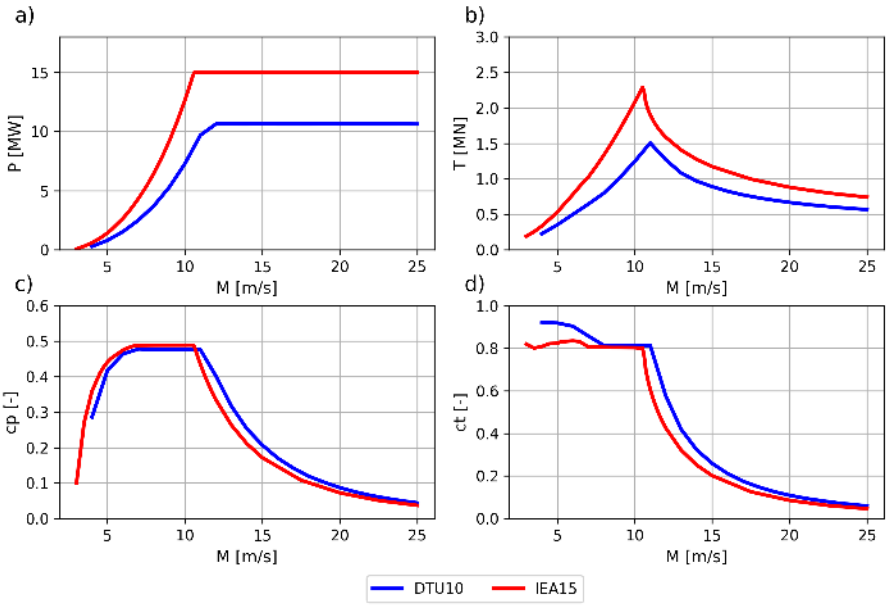

Figure 4. Power and thrust curves for the DTU10 and IEA15 wind turbines.

4 Results

4.1 Overall production numbers

The overall, year-round production statistics for the IJmuiden Ver wind farm are summarized in Table 2. Numbers are presented for the free-stream production, for the scenario with IJmuiden Ver in isolation, and for the scenario which includes the surrounding wind farms. The impact of the neighboring wind farms on the IJmuiden Ver production is highlighted by the bold numbers. The results indicate that for the simulated year the energy production of IJmuiden Ver is 701 GWh (or 3.9%) lower when including the impact of the surrounding parks.

Metric	Free-stream	IJVer Isolated	With all windfarms
Power/turbine [MW]	9.44	7.75	7.45
Production [GWh]	22166	18183	17482
Loss w.r.t. free stream [GWh]	0	3982	4683
Loss w.r.t. isolated [GWh]	-	0	**701**
Loss w.r.t. free stream [%]	0.0	18.0	21.1
Loss w.r.t. isolated [%]	-	0.0	**3.9**

Table 2. Simulated production numbers for the IJmuiden Ver wind farm zone for the year 2015 for the three scenarios.

To obtain further insight into the production numbers, Figure 5 presents the turbine-averaged production as a function of the free-stream disk-averaged wind speed. Data from all wind directions are included. Generally, for strong wind conditions (disk-averaged wind speeds of 14 m/s and higher) the wind farm operates at rated power. In that case no internal wake losses occur and the impact of neighboring parks is negligible. For this wind regime, the wind turbine thrust curves decrease rapidly with increasing wind speed (Figure 4). Internal wake losses are most important in the steep part of the power curve (roughly between 6 and 12 m/s). As shown by Figure 5c, for this wind speed regime also the impact of the neighboring farms is at its maximum.

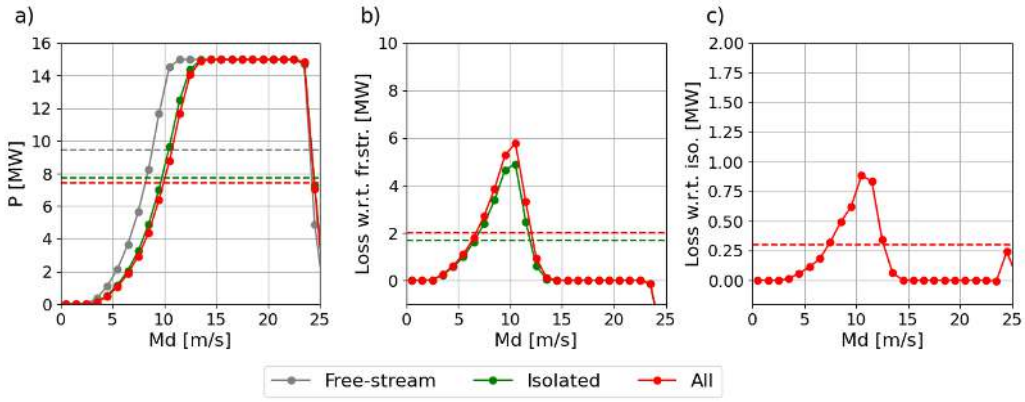

Figure 5. Turbine-averaged IJmuiden Ver power statistics as a function of free-stream disk-averaged wind speed. a) Year-averaged production per turbine. b) Production loss (per turbine) of *SIM-ISO* and *SIM-ALL* with respect to the free-stream prodcution (*SIM-FS*). c) Production loss (per turbine) of *SIM-ALL* with respect to *SIM-ISO*. Dashed lines indicate the average values over all wind speeds.

Figure 6 presents the production losses from a relative perspective. Data from all wind directions are included. The overall losses with respect to *SIM-FS* are 18.0% for *SIM-ISO* and 21.1% for *SIM-ALL*. For strong wind speeds, losses are negligible, but they rapidly increase to more than 40% when the production drops below rated power. While the negative impact of the neighboring parks is almost 4% on average, for lower wind (where most of the actual losses occur) this number increases to around 10% (Figure 6b). For wind speeds lower than 4 m/s no data are shown as the absolute production numbers become negigible (Figure 5). The values around the cut-out wind speed result from small differences in the wind field between the two simulations causing more or less turbines either producing at rated power or zero power. In an absolute sense the impact of this feature is small as the frequency of occurrence of these strong wind speeds is low (Fig. 2b).

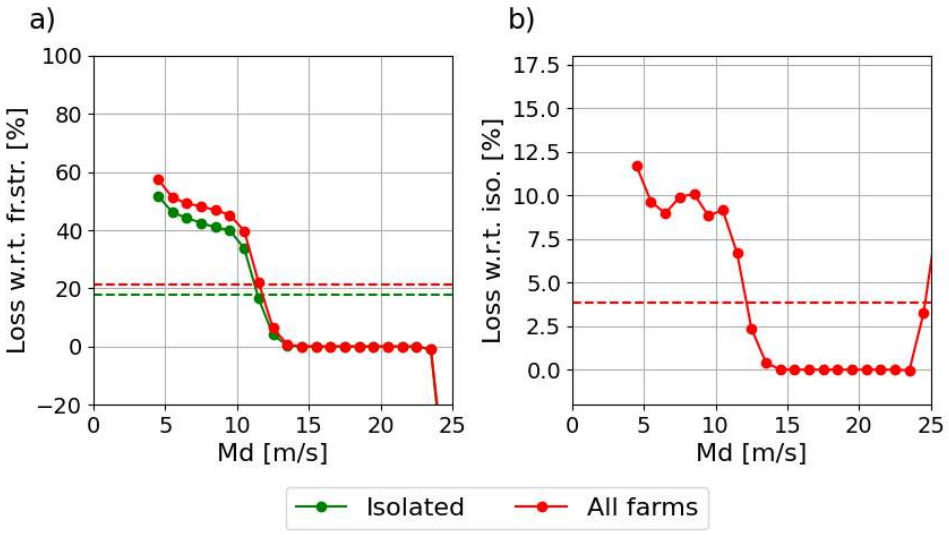

Figure 6. Relative production losses with repect to *SIM-FS* (a) and *SIM-ISO* (b) as a function of disk-averaged wind speed. Dashed lines indicate the average values over all wind speeds.

4.2 Directional effects

When considering the direction-dependency of the difference in production between the simulation with the isolated IJmuiden Ver wind farm and the simulation that includes the surrounding wind farms, the impact of individual upstream wind farms can be recognized. This is shown in Figure 7. For north-easterly winds the impact of IJmuiden Ver North is clearly visible. The same is true for Hollandse Kust West for south-easterly flow. The impact of the British wind farms in the southwest is relatively small: the distance between these wind farms and IJmuiden Ver is generally larger, their density in terms of installed MW/km2 is relatively low, and winds from the southwest tend to be stronger than for other directions (Figure 2c). For north-westerly directions the southern part of Nederwiek has a clear negative impact on the IJmuiden Ver production.

Interestingly, for specific wind direction sectors the production of IJmuiden Ver seems to be enhanced by the presence of the neighboring wind farms. In particular, this is the case for south-southwesterly and north-northwesterly flow. The increased production is associated with flow acceleration between and along the sides of the upstream wind farms (see also Section 4.5).

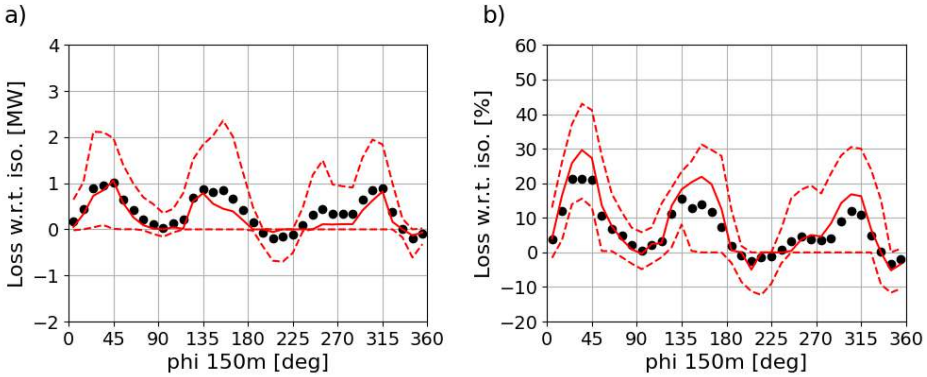

Figure 7. Direction dependency of absolute (a) and relative (b) production losses resulting from neighboring wind farms on IJmuiden Ver. Values are given per 10-degree direction bins. Black dots indicate the means, solid red lines the median values, and dashed lines the 10^{th} and 90^{th} percentiles.

4.3 Stability

Figure 7 indicates that the impact of upstream wind farms on the IJmuiden Ver production is highly variable (compare the 10th and 90th pecentiles). This is logical as for each wind direction bin the wind speed may vary significantly. And, as shown before, the losses depend highly on the wind speed itself (see Figs. 5 and 6).

Apart from the magnitude of the wind speed, another factor that impacts the strength and persistence of wind farm wakes is atmospheric stability. To study the impact of stability we define the bulk-Richardson number, R_b, over the rotor blade of the IEA15 turbine, i.e. between heights of 270 and 30 m:

$$R_b = \frac{g}{\overline{\vartheta_l}} \frac{\Delta z \Delta \vartheta_l}{(\Delta u)^2 + (\Delta v)^2}$$

.

We consider three classes of stability, separated by the 33.3$^{\text{th}}$ and 66.6$^{\text{th}}$ percentiles of the year-round distribution of R_b, which have values of 0.02 and 0.23, respectively. As such, the stability class with the 33.3% of lowest R_b values represents (mostly) unstable conditions, while the class with the 33.3% of highest R_b values represents significantly stable conditions. The class of intermediate stability contains neutral conditions, but is dominated by weakly-stratified conditions.

For assessing the impact of stability on production losses due to wind farm wakes, we only include wind direction sectors with upstream wind farms. Based on Figs. 3 and 7, three of these sectors are identified: $10° < phi < 60°$, $120° < phi < 170°$, and $250° < phi < 330°$. Together these contain 45 % of the data.

For the disturbed wind direction sectors, Fig. 8 shows the difference in turbine-averaged production between *SIM-ISO* and *SIM-ALL* for the three stability classes as a function of free-stream disk-averaged wind speed. Again, the strongest impact of upstream wind farms occurs for wind speeds around 10 m/s. A very clear impact of stability is visible with a much higher impact for stably-stratified conditions than for unstable conditions. Our results suggest that wind farm wakes may cause a 20 % reduction in energy production in significantly stably-stratified conditions for wind speeds up till 12 m/s (Fig. 8b).

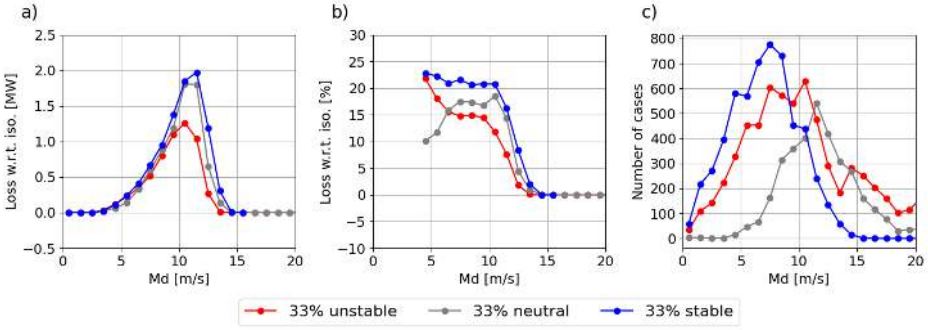

Figure 8. Absolute (a) and relative (b) production difference between the simulation with only IJmuiden Ver and the simulation including all wind farms as a function of disk-averaged wind speed. Colors indicate stability classes. Only wind directions with upstream wind farms ('disturbed' wind directions) are included here.

4.4 Impact for different parts of IJmuiden Ver

So far, we discussed the impact of neighboring farms on the production the IJmuiden Ver wind farm as a whole. In practice, IJmuiden Ver will be composed of four separate sites ('kavels') with 1 GW installed capacity each (see Fig. 3). It is well possible that the impact of the upstream wind farms will vary among the four sites. Indeed, Table 3 indicates significant differences in production for the four sites. Even in the simulation with the isolated IJver wind farm (*SIM-ISO*), Kavel II (the 'southwesterly' site) produces 5 % more energy than Kavel III (the most 'northeasterly' site). This difference is because the dominant wind direction is from the southwest (Fig. 2c). The difference in the impact of the neighboring windfarms appears from the difference in production numbers between *SIM-ISO* and *SIM-ALL*. The results suggest that Kavel I (the most 'southeasterly' site) experiences the lowest impact from upstream wind farms, while for Kavel IV (the most 'northwesterly' site) the impact is largest.

For the separate sites, Fig. 9 shows the losses due to upstream wind farms for 10-degree wide direction bins. Large differences between the sites occur. For example, for northeasterly winds ($45 ° < phi < 90 °$) the presence of IJmuiden Ver North significantly reduces the production of Kavel IV, while the production of Kavel I is in fact increased by the presence of the neighboring wind farms. Not surprisingly, the impact of Hollandse Kust West is largest for the two easterly sites (Kavels I and III).

4.5 Spatial patterns

Clearly, the impact of upstream wind farms is not uniformly distributed over the IJmuiden Ver wind farm zone. To illustrate this further, we present maps of aerodynamic losses per turbine (defined as the relative loss with respect to *SIM-FS*) and mean

Metric	P_{iso} [GWh]	$P_{fs\text{-}iso}$ [GWh]	$P_{fs\text{-}iso}$ [%]	P_{all} [GWh]	$P_{iso\text{-}all}$ [GWh]	$P_{iso\text{-}all}$ [%]
Kavel I	4562	978	17.7	4435	127	2.8
Kavel II	4623	916	16.5	4478	145	3.1
Kavel III	4402	1139	20.6	4235	167	3.8
Kavel IV	4594	946	17.1	4331	263	5.7
Total	18183	3982	18.0	17482	701	3.9

Table 3. Simulated production numbers for the IJmuiden Ver wind farm zone for the year 2015 for each of the four IJmuiden Ver sites ('kavels').

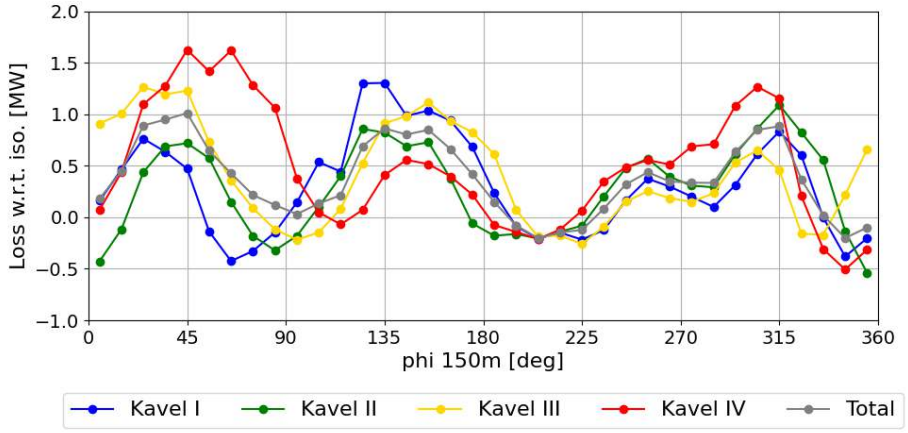

Figure 9. Turbine-averaged production losses for the four IJmuiden Ver sites as a result of upstream wind farms (*SIM-ISO* – *SIM-ALL*) as a function of wind direction.

140-m wind speed for a selection of 30-degree wind direction sectors. Figure 10 shows data for wind directions between 30 and 60 degrees. For this direction, IJmuiden Ver is in the wake of the IJmuiden Ver North wind farm. As a result, the most northerly turbines experience a large drop in production of more than 20 %. Further downstream the IJmuiden Ver wind farm the production deficit becomes smaller. Moreover, the model results suggest that the southeasterly part of the wind farm, roughly corresponding to Kavel I, experiences an increase in production as a result of the surrounding wind farms (Fig. 10c). This is a result of flow acceleration along the sides of and between IJmuiden Ver and Hollandse Kust West (Fig. 10d).

For southeasterly winds, with wind directions between 120 and 150 degrees, a clear impact of Hollandse Kust West is visible (Fig. 11). In particular for the eastern part of IJmuiden Ver the production is reduced. The mean wind field field suggests that, on its turn, wakes effect from IJmuiden Ver clearly impact the Nederwiek Zuid area.

For wind directions between 210 and 240 degrees the impact of the surrounding wind farms on the IJmuiden Ver production numbers is relatively small. This is shown in Fig. 12. Along the western part of IJmuiden Ver, a small reduction is production is predicted. The distance to the upstream British wind farms is larger than towards other neighboring wind farms. Also, the capacity density of these wind farms is relatively low.

For wind directions between 300 and 330 degrees, a clear impact of Nederwiek Zuid on the IJmuiden Ver production is visible (Fig. 13). Remarkably, the production in the northern part of IJmuiden Ver increases when taking the neighboring wind farms in to account, possibly as result of acceleration between IJmuiden Ver and IJmuiden Ver North.

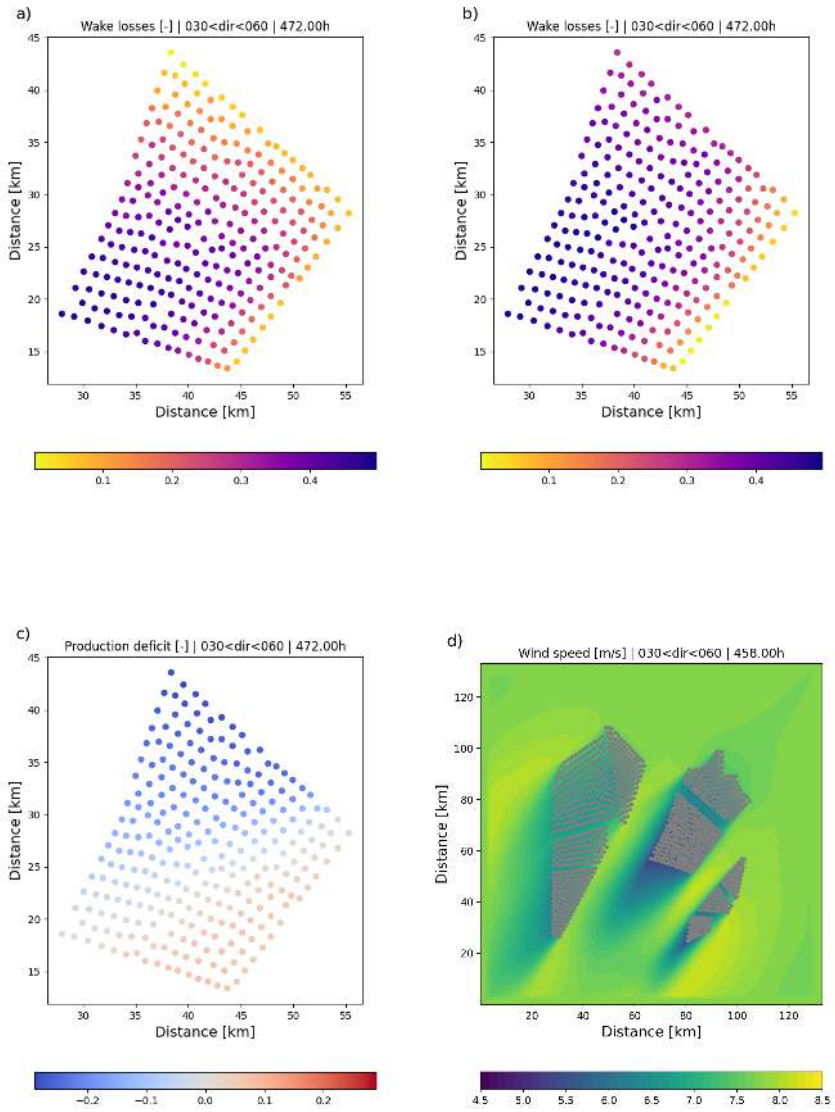

Figure 10. Composite maps of relative aerodynamic losses and 140-m wind speed for wind directions between 30 and 60 degrees. a) Production losses of the isolated IJmuiden Ver simulation with respect to the free stream production. b) Production losses of the simulation including the surrounding wind farms with respect to the free stream production. c) Production losses of the simulation including the surrounding wind farms with respect to the isolated IJmuiden Ver simulation. d) Mean 140-m wind speed for the simualtion including the surrounding wind farms.

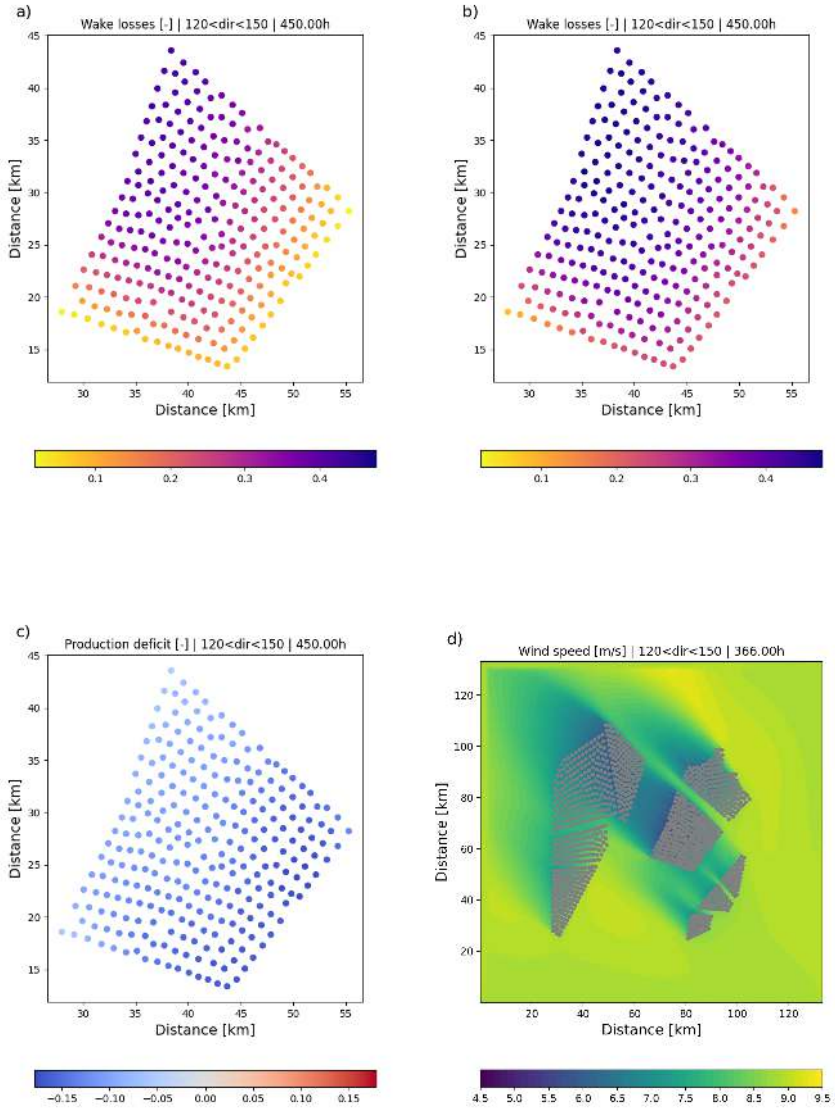

Figure 11. As Fig. 10, but for wind directions between 120 and 150 degrees.

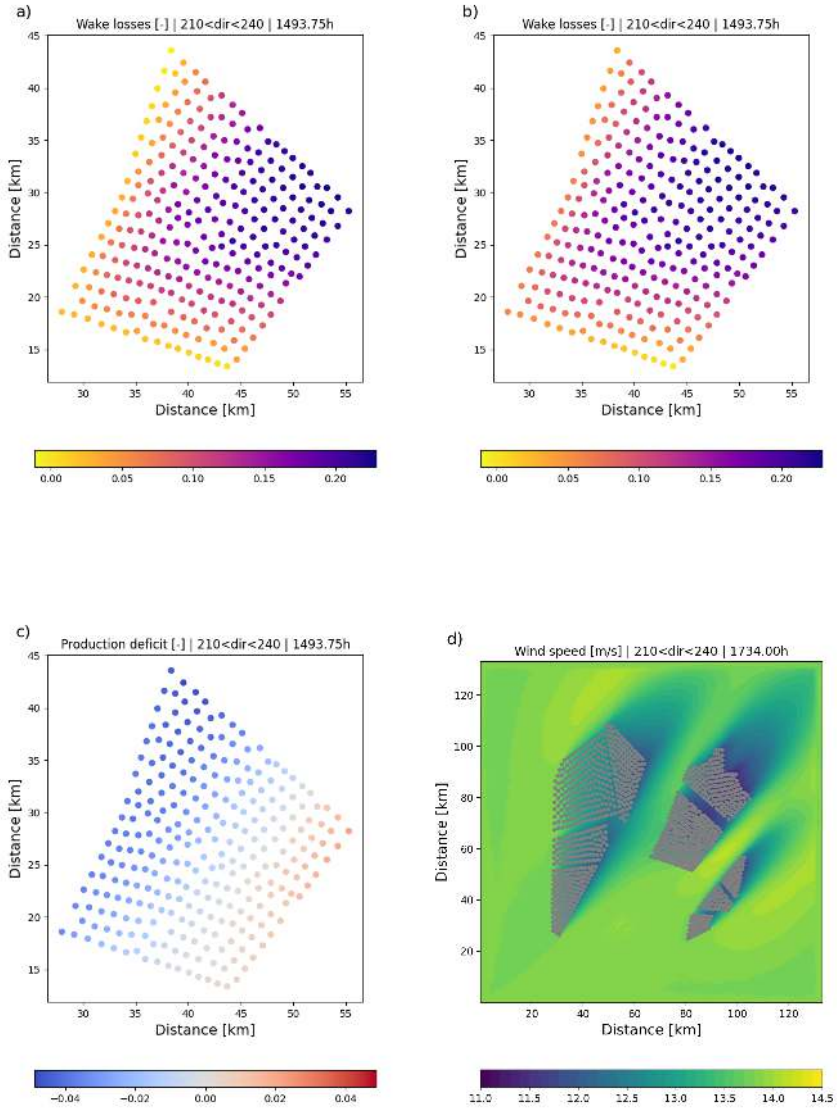

Figure 12. As Fig. 10, but for wind directions between 210 and 240 degrees.

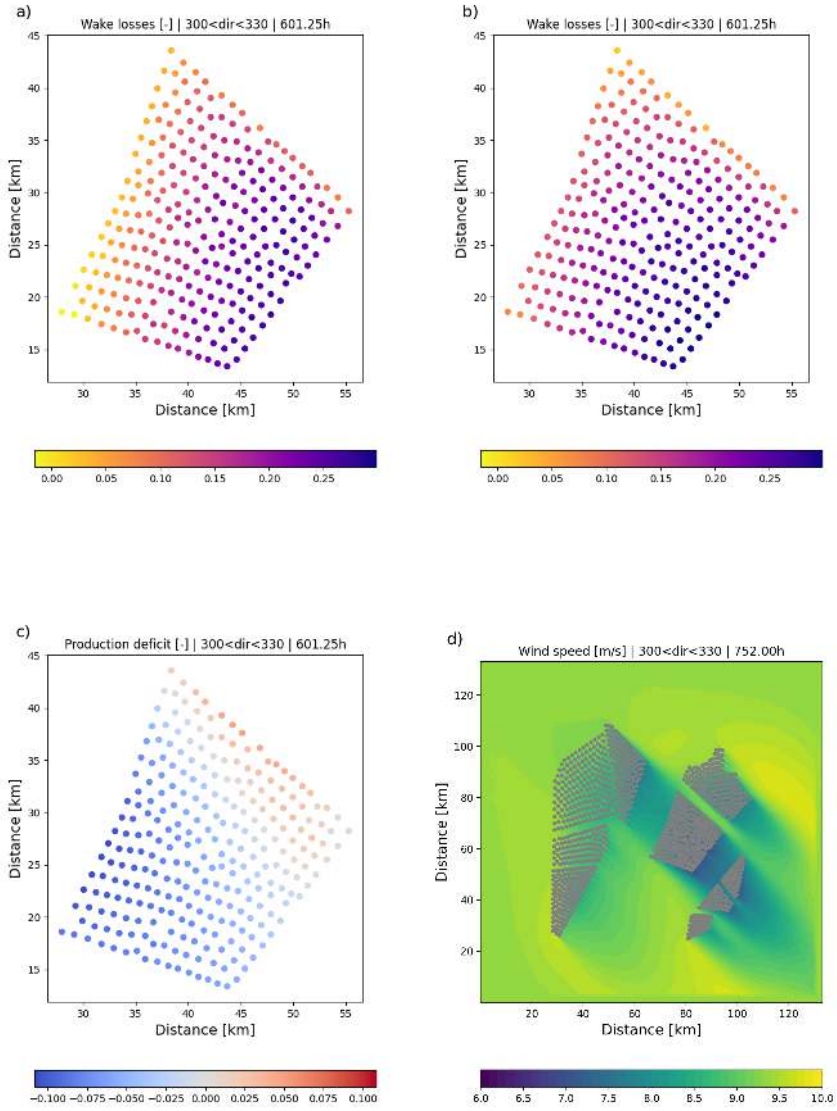

Figure 13. As Fig. 10, but for wind directions between 330 and 360 degrees.

5 Discussion

The present pilot study provides a first estimate of the potential impact of neighboring wind farms on the planned 4 GW IJmuiden Ver wind farm using atmospheric large-eddy simulation. To that end, a full year of model simulations have been performed with realistic weather conditions. In order to keep the computational costs of the simulations within reasonable limits, a relatively coarse grid-spacing of 140 m has been applied. Also, although the simulated domain extends to 143.36 km, it can be argued that this is still too small for accurately modeling the effects of the included wind farms. Therefore, although the present study gives a clear indication that surrounding wind farms will have a significant impact on the production of the IJmuiden Ver wind farm, further research is needed to characterize the impact of specific model settings. Furthermore, the presented results are valid for the year 2015. To obtain numbers that are representative from a climatological perspective a long-term correction should be applied to account for year-to-year variability.

In this respect, it is interesting to inspect model output from simulations of the HARMONIE-AROME numerical weather-prediction model that were done in the framework of the Winds of the North Sea in 2050 (WINS50) project ([Wijnant et al., 2022]). We consider two simulations that were done for the year 2020: one without the impact of wind farms ('CTL') and one which includes the impact of a hypothetical 2050 installed offshore capacity scenario (W50). In HARMONIE-AROME, wind farms are modeled using the [Fitch et al., 2012] parameterization. Although, the 2050 scenario that is used in the HARMONIE-ARMOME W50 simulation differs from the scenario applied in the present GRASP study and the simulation covers a different year, a qualitative comparison of modeled wake effects may still be insightful. Therefore, Fig. 14 shows composite velocity deficits (W50-CTL) of the 150-m wind speed for four 30-degree wide wind direction sectors (corresponding to the wind direction sectors that were shown for GRASP in Figs. 10 to 13). Figure Fig. 14 clearly shows that also in HARMONIE-AROME wakes from neighboring wind farms reach IJmuiden Ver.

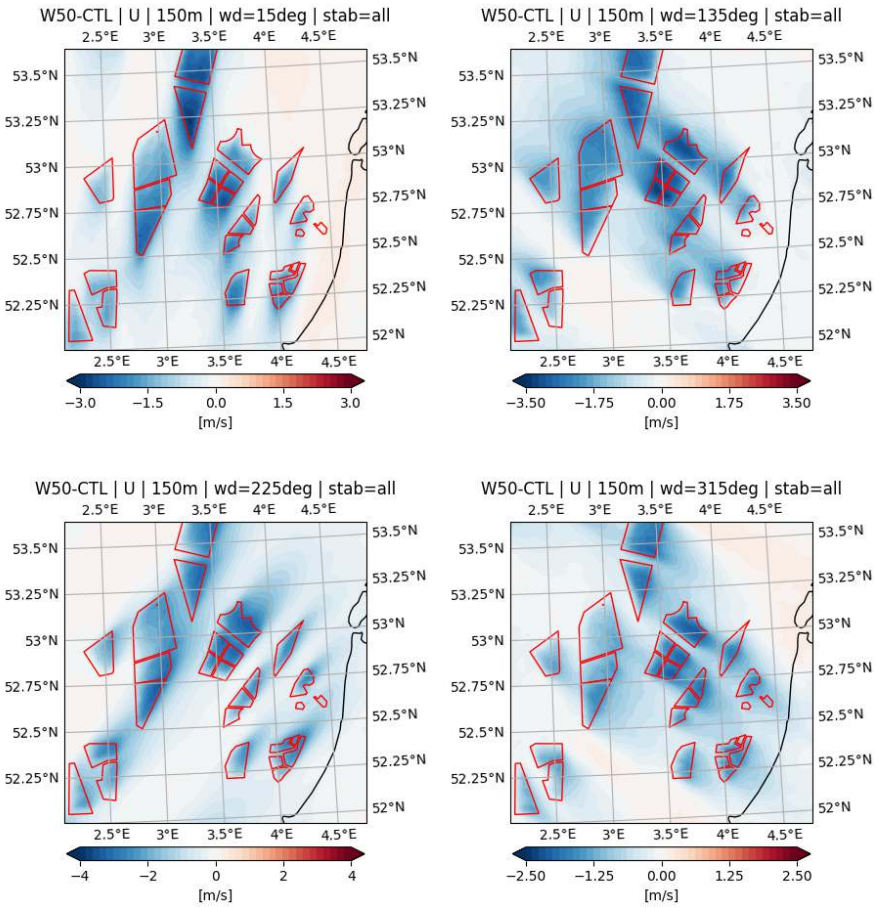

Figure 14. Velocity deficits (W50-CTL, 150-m wind speed) as modeled by HARMONIE-AROME for the year 2020 for four 30-degree wind direction sectors.

6 Conclusions

In this report we explore the potential impact of surrounding wind farms on the production of the planned 4 GW IJmuiden Ver wind farm. Therefore, we modeled one year of realistic weather with atmospheric large-eddy simulation (LES). We compared production numbers of a simulation with the IJmuiden wind farm in isolation with those of a simulation with all surrounding wind farms included. Results of both simultions were compared to free-stream production numbers.

The modeling results suggest that the energy production of the future wind farm of IJmuiden Ver may experience significant production losses from wake effects of upstream wind farms. For the simulated year of 2015 the production deficit amounts to 4 % (corresponding to 701 GWh).

For wind speeds stronger than 14 m/s the impact of surrounding wind farms is negligible. Losses due to wakes from upstream wind farms occur mainly for wind speeds between 6 and 12 m/s. For this wind speed range the omni-directional production loss as a result of neighboring farms amounts to 10 %. When only considering wind directions with upstream wind farms ('disturbed' direction sectors) the production deficit may increase to 20 % in significantly stably-stratified conditions.

The production deficits resulting from upstream wind farms show a strong dependency on wind direction, which is to be expected. For some wind directions the production of IJmuiden Ver may even increase as a result of the presence of upstream wind farms. This is the case when flow accelerations along the sides of these wind farms reach IJmuiden Ver. Inspection of the production numbers for the four separate sites ('kavels') of the IJmuiden Ver wind farm indicates that the impact of the surrounding farms shows significant spatial variations: for some wind directions one site may experience a serious reduction in energy production, while one of the other sites may in fact show an increase in production.

Inspection of spatial fields reveals complex patterns of both wind farm wakes and flow accelerations along the sides of individual wind farms. The turbine-level model output of GRASP allows for a detailed analysis of variations of energy production over the wind farm.

The results of this explorative study suggest that with the rapid increase of offshore wind energy capacity farm-to-farm interactions cannot be ignored. As such, the effect of upstream wind farms must be taken into account in annual energy production assessments for present-day and future wind farms.

References

Baas et al., 2022. Baas, P., Verzijlbergh, R., Van Dorp, P., and Jonker, H. (2022). Investigating energy production and wake losses of multi-gigawatt offshore wind farms with atmospheric large-eddy simulation. *Wind Energy Science Discussions*.

Calaf et al., 2010. Calaf, M., Meneveau, C., and Meyers, J. (2010). Large eddy simulation study of fully developed wind-turbine array boundary layers. *Physics of Fluids*, 22:1–16.

European Commission, 2020. European Commission (2020). Offshore renewable energy strategy.

Fitch et al., 2012. Fitch, A., Olson, J., Lundquist, J., Dudhia, J., Gupta, A., Michalakes, J., and Barstad, I. (2012). Local and mesoscale impacts of wind farms as parameterized in a mesoscale NWP Model. *Mon Weather Rev*, 140:3017–3038.

Hasager et al., 2015. Hasager, C., Vincent, P., Badger, J., Badger, M., Di Bella, A., Peña, A., Husson, R., and Volker, P. (2015). Using Satellite SAR to Characterize the Wind Flow around Offshore Wind Farms. *Energies*, 8:5413–5439.

Hersbach et al., 2020. Hersbach, H., Bell, B., P., B., Hirahara, S., Horányi, A., Muñoz-Sabater, J., Nicolas, J., Peubey, C., Radu, R., Schepers, D., Simmons, A., Soci, C., Abdalla, S., Abellan, X., Balsamo, G., Bechtold, P., Biavati, G., Bidlot, J., Bonavita, De Chiara, G., Dahlgren, P., Dee, D., Diamantakis, M., Dragani, R., Flemming, J., Forbes, R., Fuentes, M., Geer, A., Haimberger, L., Healy, S., Hogan, R., Hólm, E., Janisková, M., Keeley, S., Laloyaux, P., Lopez, P., Lupu, C., Radnoti, G., De Rosnay, P., Rozum, I., Vamborg, F., Villaume, S., and Thépaut, J. (2020). The ERA5 global reanalysis. *Quarterly Journal of the Royal Meteorological Society*, 146:1999–2049.

Heus et al., 2010. Heus, T., Van Heerwaarden, C. C., Jonker, H. J. J., Siebesma, A. P., Axelsen, S., Van Den Dries, K., Geoffroy, O., Moene, A. F., Pino, D., De Roode, S. R., and Vila-Guerau de Arellano, J. (2010). Formulation of the Dutch Atmospheric Large-Eddy Simulation (DALES) and overview of its applications. *Geoscientific Model Development*, 3(2):415–444.

Lundquist et al., 2019. Lundquist, J., DuVivier, K., Kaffine, D., and Tomaszewski, J. (2019). Costs and consequences of wind turbine wake effects arising from uncoordinated wind energy development. *Nature Energy*, 4:26–34.

Maas and Raasch, 2022. Maas, O. and Raasch, S. (2022). Wake properties and power output of very large wind farms for different meteorological conditions and turbine spacings: A large-eddy simulation case study for the german bight. *Wind Energy Science*, 7:715–739.

Meyers and Meneveau, 2010. Meyers, J. and Meneveau, C. (2010). Large Eddy Simulations of Large Wind-Turbine Arrays in the Atmospheric Boundary Layer. *48th AIAA Aerospace Sciences Meeting Including the New Horizons Forum and Aerospace Exposition*, (January):1–10.

Platis et al., 2018. Platis, A., Siedersleben, S., Bange, J., Lampert, A., Bärfuss, K., Hankers, R., Cañadillas, B., Foreman, R., Schultz-Stellenfleth, J., Djatj, B., Neumann, T., and Emeis, S. (2018). First in situ evidence of wakes in the far field behind offshore wind farms. *Nature Scientific Reports*, 8:2163.

Rijksoverheid, 2021. Rijksoverheid (2021). Additional Draft North Sea Programme 2022-2027. Technical report.

RVO, 2022. RVO (2022). General information IJmuiden Ver.

Schalkwijk et al., 2012. Schalkwijk, J., Griffith, E. J., Post, F. H., and Jonker, H. J. J. (2012). High-performance simulations of turbulent clouds on a desktop PC. *Bulletin of the American Meteorological Society*, 93(3):307–314.

Schalkwijk et al., 2015. Schalkwijk, J., Jonker, H. J. J., Siebesma, A. P., and Bosveld, F. C. (2015). A Year-Long Large-Eddy Simulation of the Weather over Cabauw: an Overview. *Monthly Weather Review*, 143:828–844.

Schneemann et al., 2020. Schneemann, J., Rott, A., Dörenkämper, M., Steinfeld, G., and Kühn, M. (2020). Cluster wakes impact on a far-distant offshore wind farm's power. *Wind Energy Science*, 5:29–49.

Stevens et al., 2014. Stevens, R. J., Graham, J., and Meneveau, C. (2014). A concurrent precursor inflow method for Large Eddy Simulations and applications to finite length wind farms. *Renewable Energy*, 68:46–50.

The Esbjerg Declaration, 2022. The Esbjerg Declaration (2022). The esbjerg declaration on the north sea as a green power plant of europe.

Wijnant et al., 2022. Wijnant, I. L., Theeuwes, N., Van Ulft, B., Zoer, T., and Baas, P. (2022). Wind farms in WINS50 climatology. Technical report.

Witkin and Heckbert, 2005. Witkin, A. and Heckbert, P. (2005). Using particles to sample and control implicit surfaces. In *ACM SIGGRAPH 2005 Courses*.